様　式　Ｃ－１９、Ｆ－１９、Ｚ－１９　（共通）

科学研究費助成事業　　研究成果報告書

平成 ２６ 年　 ６ 月　 ９ 日現在

機関番号：８２１１０
研究種目：若手研究(B)
研究期間：2011～2013
課題番号：２３７４０４１３
研究課題名（和文）New high harmonic generation mechanism

研究課題名（英文）New high harmonic generation mechanism

研究代表者
ＰＩＲＯＺＨＫＯＶ　Ａｌｅｘ（Pirozhkov, Alexander）

独立行政法人日本原子力研究開発機構・原子力科学研究部門　量子ビーム応用研究センター・研究副主幹

研究者番号：００４４６４１０

交付決定額（研究期間全体）：（直接経費）　　3,000,000円、（間接経費）　　900,000円

研究成果の概要（和文）：マルチテラワットのフェムト秒レーザーをガスジェットに1e18 W/cm2 以上の集光強度で照射することで発生する新しい高次高調波について研究を行った。高調波のスペクトル特性、放射の角度依存性、コヒーレンス性、そして光源サイズを決定し、原子力機構の9 TWのレーザーJ-KARENを用いて、高調波のエネルギーが水の窓領域である360 eVへ至ることを観測した。さらに、このような高調波の生成機構として、形成された密度特異点の電子スパイクが振動することで発生するという新しいモデルを提案し、それを確認した。
この結果は、次世代の明るくコンパクトでコヒーレントなX線源として、新たな方向性を示すものである。

研究成果の概要（英文）：I studied a new regime of high-order harmonic generation in the interaction of multi-terawatt femtosecond lasers focused up to intensity I_0>1e18 W/cm2 into gas jet targets. I determined spectral properties, angular distribution, coherence, and source size. In experiments with the 9 TW J-KAREN laser in Japan Atomic Energy Agency (JAEA), the photon energy of harmonic radiation reached 360 eV, within the "water window" spectral region. I suggested and justified a new model of harmonic generation by relativistic electron spikes, which are density singularities resulting from catastrophes of a multi-stream relativistic plasma flow.
The results may open a way toward a next-generation bright compact coherent x-ray source which can be built on a university-lab-scale repetitive laser and accessible, replenishable, debris-free gas jet target. This will impact many areas of fundamental research and applications requiring a bright x-ray source for pumping, probing, imaging, or attosecond science.

研究分野：数物系科学

科研費の分科・細目：プラズマ科学・プラズマ科学

キーワード：プラズマ制御　レーザー

１．研究開始当初の背景 Background

Surprisingly, I experimentally found strong forward harmonics when a relativistic laser (intensity $I_0 > 10^{18}$ W/cm^2, pulse duration $\tau < 100$ fs) irradiated He gas jet. In contrast to atomic harmonics, both odd and even orders were observed; the harmonics were generated by linearly as well as circularly polarized pulses. However, other properties of these harmonics and their origin were not clear.

２．研究の目的 Purpose

The research purpose was to clarify angular distribution, coherence, and source size of the newly discovered harmonics and determine possible applications.

３．研究の方法 Methods

I employed the relativistic regime of laser-plasma interaction [Mourou et al., *Rev. Mod. Phys.* **78** 309 (2006)]. In this regime, the dimensionless laser pulse amplitude $a_0 \approx 0.85\lambda_{\mu m} I_{18}^{1/2}$ is larger than 1. Here $\lambda_{\mu m}$ is laser wavelength in μm and I_{18} is intensity in 10^{18} W/cm^2.

I focused multi-terawatt (peak power $P_0 \approx$ 10-200 TW) femtosecond (pulse duration $\tau \approx$ 30-60 fs) laser pulses to helium gas jet targets (interaction length ~1 mm, density n_e ~10^{19} cm^{-3}) to generate extreme ultraviolet (XUV) and soft x-ray harmonics (wavelength 3.4 to 30 nm, photon energy $\hbar\omega$ = 40 to 360 eV). The relativistic self-focusing effect [Mourou et al., *Rev. Mod. Phys.* **78** 309 (2006)] additionally enhanced the laser intensity in plasma up to I_{SF} ~ 10^{19} – 10^{20} W/cm^2.

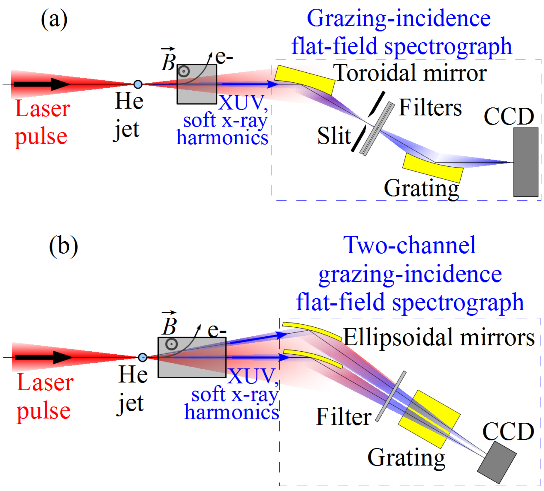

Figure 1. Experimental setup schematics for relativistic high-order harmonic generation in gas jet targets, with (a) single-channel grazing-incidence spectrograph, (b) two-channel grazing-incidence spectrograph. [Pirozhkov et al., *SPIE* **8140**, 81400A-16 (2011)].

The experiments had been performed with the J-KAREN laser (KPSI, JAEA, Japan) and Astra Gemini laser (CLF, RAL, UK). The experimental setup schematics are shown in Figure 1. I used absolutely calibrated (Figure 2, Figure 3) single-channel and multi-channel (Figure 4) flat-field spectrographs as well as wide-acceptance-angle spectrograph to measure the spectral properties and angular distribution of the harmonics. I used mesh diffraction and high-resolution imaging to estimate the harmonics coherence and source size.

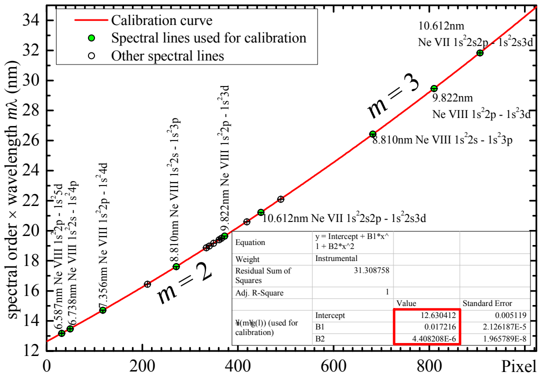

Figure 2. Example of wavelength calibration.

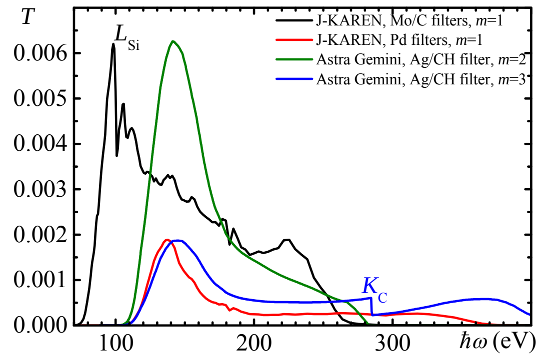

Figure 3. Spectrograph throughputs.

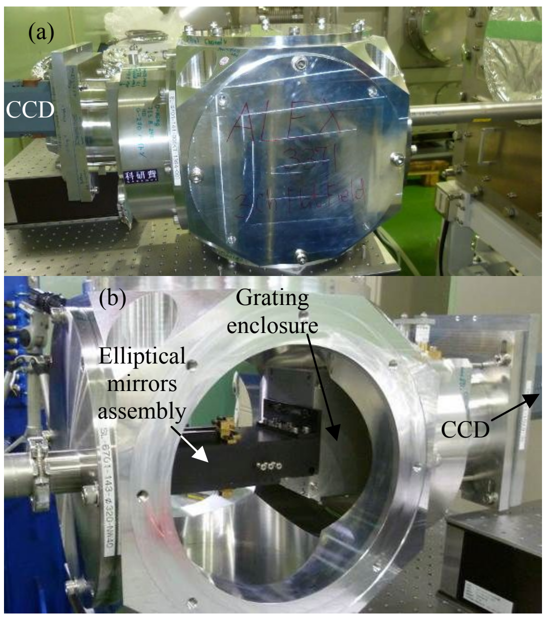

Figure 4. Multi-channel flat field spectrograph. (a) Assembled, (b) opened.

4．研究成果 Results

The high-frequency harmonic radiation with photon energy up to $\hbar\omega$ = 360 eV (corresponding to the spectrograph limit) was observed in the interaction of laser pulses (either linearly or circularly polarized) with power from P_0 = 9 to 170 TW and helium gas jets with the electron density from $n_e = 1.7\times10^{19}$ to 7×10^{19} cm^{-3}.

Spectral properties

The comb-like spectra comprising odd and even harmonics of similar intensity and shape were generated in the broad range of laser and plasma parameters, demonstrating the effect's robustness. Typical spectra obtained with linearly polarized laser pulses are shown in Figure 5 and Figure 6. A spectrum obtained with the circularly polarized laser pulse is shown in Figure 7.

The base frequency of the spectra, ω_f, was downshifted from the laser frequency, ω_0, due to the well-known gradual frequency downshift of a laser pulse propagating in tenuous plasma [Bulanov et al., *Phys. Fluids B* **4**, 1935 (1992)]. Harmonics up to the order ~370th were distinguishable, e.g. in the shot shown in Figure 7.

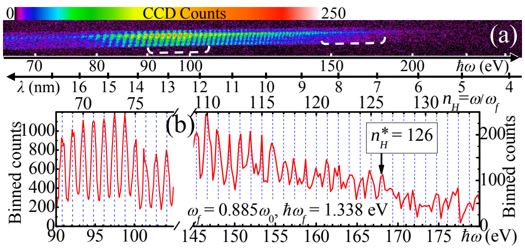

Figure 5. Harmonic spectrum obtained with the laser power P_0 = 9 TW, linear polarization, and peak electron density $n_e = 2.7\times10^{19}$ cm^{-3}. (a) Raw data. (b) The lineouts of two selected regions, brackets in (a). [Pirozhkov et al., *Phys. Rev. Lett.* **108**, 135004 (2012)].

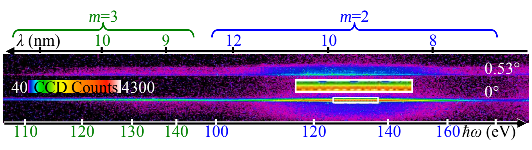

Figure 6. Harmonic spectrum obtained with P_0 = 120 TW, linear polarization, $n_e = 1.9\times10^{19}$ cm^{-3}. The top and bottom spectra correspond to the 0.53° off-axis and on-axis channels, respectively. The inset shows magnified portion of the on-axis spectrum. The spectrograph operates in the 2nd and 3rd diffraction orders, *m*. The spectrum of the on-axis channel is shown in Figure 8 by blue (*m*=2) and green (*m*=3) lines. [Pirozhkov et al., *SPIE* **8140**, 81400A-16 (2011)].

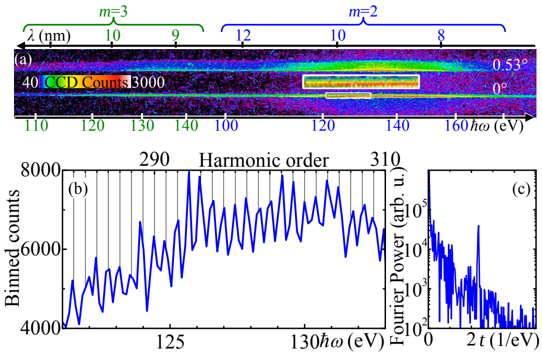

Figure 7. Harmonic spectrum obtained with P_0 = 170 TW, circular polarization, $n_e = 4\times10^{19}$ cm^{-3}. (a) Raw data and magnified portion (inset). (b) Lineout corresponding to the inset in (a). (c) Fourier transformation of the spectrum in the spectral range from 120 to 160 eV. The clear narrow peak at 2.33 eV^{-1} corresponding to $\hbar\omega_f$ = 0.429 eV shows spectrum periodicity. [Pirozhkov et al., *SPIE* **8140**, 81400A-16 (2011)].

Photon yield

A remarkable feature of the harmonic spectra was their high brightness, so that each of the spectra shown was the result of single-shot acquisition. The harmonic pulse energy and photon numbers were conservatively estimated using spectrograph throughputs, Figure 3. Examples of the spectra in the units of μJ/(eV·sr) are shown in Figure 8 and Figure 9. The photon yield scaled favourably with the laser power, as follows from the comparison of the harmonic spectra obtained with the 9 TW and 120 TW laser powers, Figure 8.

At 120 TW laser power, the harmonic pulse energy and photon number in a unit solid angle reached 40 μJ/sr and 2×10^{12} photons/sr in one harmonic at 120 eV. Assuming 3° angular width derived from the simulations (see below), these amount to 90 nJ pulse energy and 4×10^9 photons.

The harmonic emission extended up to the 'water window' spectral range, Figure 9. Within the 'water window' the spectrum contained ~0.8 μJ/sr pulse energy or ~1.5×10^{10} photons/sr. For the assumed 3° angular width, these correspond to 1.7 nJ and 3×10^7 photons.

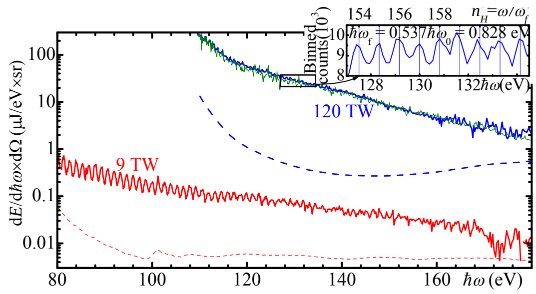

Figure 8. Comparison of the spectra obtained with the 9 TW (Figure 5) and 120 TW (Figure 6) lasers. The dashed curves indicate the noise level. [Pirozhkov et al., *Phys. Rev. Lett.* **108**, 135004 (2012)].

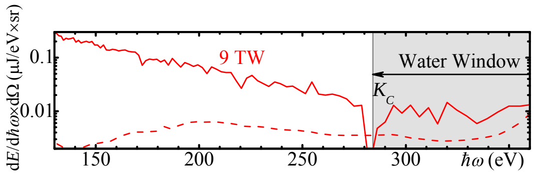

Figure 9. The spectrum within the 'water window' spectral region obtained with the 9 TW laser, linear polarization, $n_e = 4.7\times10^{19}$ cm^{-3}. The dashed curve indicates the noise level. [Pirozhkov et al., *Phys. Rev. Lett.* **108**, 135004 (2012)].

Angular distribution

Two spectrograph channels observing the harmonics on-axis and 0.53° off-axis, Figure 6 and Figure 7, showed spectra with similar intensity, taking into account 2.5-fold difference in acceptance angles. This indicated that the angular distribution of the harmonic emission has a characteristic size of several degrees.

I also measured angular distribution of off-axis harmonics at the observation angles from 8 to 18° using wide-acceptance-angle spectrograph in the 60 to 100 eV photon energy range [Pirozhkov et al., CLEO-QELS QW1A.3 (2013)].

The high-resolution 2D Particle-In-Cell (PIC) simulations performed with the code REMP [Esirkepov *Comput. Phys. Comm.* **135**, 144 (2001)] showed that the harmonics are emitted slightly off-axis and for harmonic orders about hundred their angular span is ~3°. The angular distribution of harmonics is shown in Figure 10.

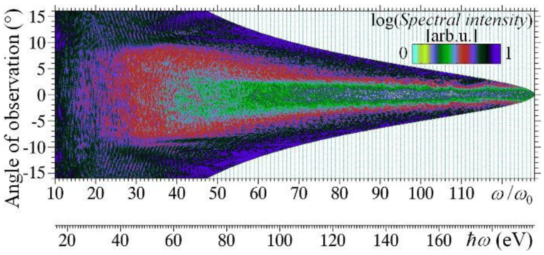

Figure 10. Angular distribution of spectral intensity corresponding to the simulation shown in Figure 13. The white area is beyond the simulation resolution. [Pirozhkov et al., "High order harmonics from relativistic electron spikes," *New J. Phys.* (submitted)].

Coherence properties

The temporal coherence of the radiation followed from the spectral fringes at the harmonic frequencies.

The spatial coherence of the harmonics was studied by the diffractive imaging method employing a sub-μm resolution, high dynamic range LiF film detector sensitive to photons with energy greater than 14 eV [Pikuz et al., *Opt. Express* **20**, 3424 (2012)]. A portion of the photoluminescent mesh shadow containing clear fringes is shown in Figure 11 (a).

Comparison of experimental and modelled diffraction patterns [Pikuz, Faenov, Pirozhkov, et al., *Phys. Status Solidi C* **9** 2331 (2012)] assuming fully coherent harmonic source, Figure 11 (b), showed that the harmonics are spatially coherent.

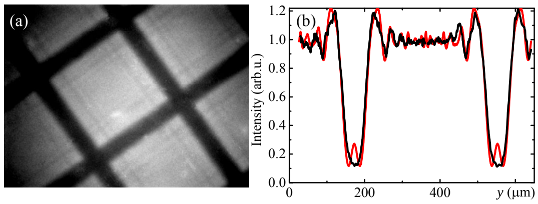

Figure 11. (a) Diffractive image of a mesh with the 362.8 μm period and 41 μm wire thickness irradiated with harmonics at the angle of 8° from the laser propagation direction; plasma-mesh distance is 550 mm, mesh-detector distance is 27.2 mm. (b) Comparison of the experimental intensity lineout (black line) with the modelled one (red line). [Pikuz, Faenov, Pirozhkov et al., *Physica Status Solidi C* **9**, 2331 (2012)].

Source size

Using normal-incidence mirror with broadband aperiodic multilayer coating, I imaged XUV (60 to 100 eV) harmonic source onto sub-μm resolution LiF detector and observed [Pirozhkov et al., CLEO-QELS QW1A.3 (2013)] that harmonic source size was much smaller than micrometer (~0.2 μm); I also observed double point source structure, as predicted by the newly developed harmonic generation model, see below.

New harmonic generation model

On the basis of the experimental data, extensive simulations, and mathematical catastrophe theory [Poston and Stewart, *Catastrophe theory and its applications* Dover Pubns, Mineola, NY, (1996)] we suggested and justified a novel model of harmonic generation by the relativistic electron spike (density singularity), Figure 12 [Pirozhkov et al., *Phys. Rev. Lett.* **108**, 135004 (2012)].

According to the model, the extremely intense laser pulse self-focuses in plasma, produces the bow wave [Esirkepov et al., *Phys. Rev. Lett.* **101**, 265001 (2008)], and makes electron-free cavity [Pukhov and Meyer-ter-Vehn, Appl. Phys. B **74**, 355 (2002)]. The bow wave boundary and cavity wall are density singularities appearing due to the folding of the phase space, i.e. *fold* catastrophes, Figure 12 (b).

The electron density spike is the higher-order *cusp* catastrophe, which exists at the joining of the two folds. The cusp catastrophe is structurally stable, which guarantee robustness of the electron spike and harmonic emission against perturbations. The density distribution, cusp formation, and harmonic emission in 2D PIC simulation are shown in Figure 13.

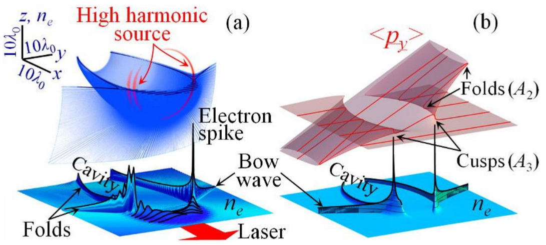

Figure 12. (a) 3D PIC simulation results showing distribution of the electron density n_e. The red arcs show the energy density of electromagnetic radiation with $\omega > 4\omega_0$, i.e. the location of the high-order harmonics source. (b) The catastrophe theory model. The upper surface is the electron phase space $(x,y,\langle p_y \rangle)$, where $\langle p_y \rangle$ is the transverse momentum averaged over the laser period. The bottom surface shows the electron density distribution with singularities corresponding to the folds of the phase space. The electron density spikes appear at the places of joining of two folds, where the higher-order cusp singularities are formed. [Pirozhkov et al., *Phys. Rev. Lett.* **108**, 135004 (2012)].

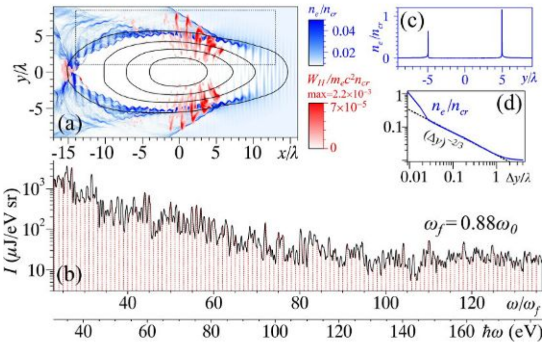

Figure 13. 2D PIC simulation results. (a) The electron density n_e (blue color scale), isolines of the laser pulse envelope for the amplitudes $a_0 = 1$, 4, 7, 10, and electromagnetic energy density W_H for frequencies from $60\omega_0$ to $100\omega_0$ (red color scale). (b) Emission spectrum of the upper spike, black dotted rectangle in (a). (c) The electron spike shape 10 laser cycles earlier than shown in (a). (d) Profile of the right spike in (c) in the log-log scale. [Pirozhkov et al., *Phys. Rev. Lett.* **108**, 135004 (2012)].

Harmonic generation scalings

Using simplified model of the cusp structure as a point source, stationary self-focusing condition, and classical electrodynamics, we obtained [Pirozhkov et al., *Phys. Rev. Lett.* **108**, 135004 (2012)] that $n_{\rm Hmax} \approx P_0 n_e / P_c n_{cr} \approx 500 P_{\rm PW} n_{19} \lambda_{\mu m}^2$, where $n_{\rm Hmax}$ is the maximum harmonic order, P_0 is laser pulse power, $P_{\rm PW}$ is laser power in petawatts, $P_c \approx 17$ GW, n_e is plasma density, n_{19} is density in 10^{19} cm^{-3}, $n_{cr} \approx 1.7\times10^{21}$ cm$^{-3}/\lambda_{\mu m}^2$ is critical density, and $\lambda_{\mu m}$ is laser wavelength in micrometers.

The total energy emitted by the spike is proportional to the electron number squared and $P_0^{4/3}$.

Possible applications

Our results open the way to a compact coherent x-ray or XUV source built on a university laboratory scale repetitive laser and an accessible, replenishable, and debris-free gas jet target. This will impact many areas requiring a bright compact x-ray or XUV source for pumping, probing, imaging, or attosecond science.

５．主な発表論文等 Main publications

〔雑誌論文〕（計　7　件）Journal papers

①.H. Kiriyama, T. Shimomura, M. Mori, Y. Nakai, M. Tanoue, S. Kondo, S. Kanazawa, A. S. Pirozhkov, T. Zh. Esirkepov, Y. Hayashi, K. Ogura, H. Kotaki, M. Suzuki, I. Daito, H. Okada, A. Kosuge, Y. Fukuda, M. Nishiuchi, M. Kando, S. V. Bulanov, K. Nagashima, M. Yamagiwa, K. Kondo, A. Sugiyama, P. R. Bolton, S. Matsuoka, and H. Kan, "Ultra-Intense, High Spatio-Temporal Quality Petawatt-Class Laser System and Applications," *Applied Sciences* **3** (1), 214-250 (2013) (Refereed paper).
DOI:10.3390/app3010214

②.T. Pikuz, A. Faenov, A. Pirozhkov, A. Astapov, G. Klushin, S. Pikuz, N. Nagorskiy, S. Magnitskiy, T. Esirkepov, J. Koga, T. Nakamura, S. Bulanov, Y. Fukuda, Y. Hayashi, H. Kotaki, Y. Kato, and M. Kando, "High performance imaging of relativistic soft X-ray harmonics by sub-micron resolution LiF film detectors," *Physica Status Solidi C* **9** (12), 2331-2335 (2012) (Refereed paper).
DOI:10.1002/pssc.201200390

③.S. V. Bulanov, T. Zh Esirkepov, M. Kando, J. K. Koga, A. S. Pirozhkov, T. Nakamura, S. S. Bulanov, C. B. Schroeder, E. Esarey, F. Califano, and F. Pegoraro, "On the breaking of a plasma wave in a thermal plasma. I. The structure of the density singularity," *Phys. Plasmas* **19** (11), 113102-7 (2012) (Refereed paper)
DOI:10.1063/1.4764056

④.S. V. Bulanov, T. Zh. Esirkepov, M. Kando, J. K. Koga, A. S. Pirozhkov, T. Nakamura, S. S. Bulanov, C. B. Schroeder, E. Esarey, F. Califano, and F. Pegoraro, "On the breaking of a plasma wave in a thermal plasma. II. Electromagnetic wave interaction with the breaking plasma wave," *Phys. Plasmas* **19** (11), 113103-7 (2012) (Refereed paper).
DOI:10.1063/1.4764052

⑤.A. S. Pirozhkov, M. Kando, T. Zh. Esirkepov, P. Gallegos, H. Ahmed, E. N. Ragozin, A. Ya. Faenov, T. A. Pikuz, T. Kawachi, A. Sagisaka, J. K. Koga, M. Coury, J. Green, P. Foster, C. Brenner, B. Dromey, D. R. Symes, M. Mori, K. Kawase, T. Kameshima, Y. Fukuda, L. M. Chen, I. Daito, K. Ogura, Y. Hayashi, H. Kotaki, H. Kiriyama, H. Okada, N. Nishimori, T. Imazono, K. Kondo, T. Kimura, T. Tajima, H. Daido, P. Rajeev, P. McKenna, M. Borghesi, D. Neely, Y. Kato and S. V. Bulanov, "Relativistic high harmonic generation in gas jet targets," [invited] *AIP Conf. Proc.* **1465**, 167-171 (2012) (Proc. The 3rd International Symposium "Laser-Driven Relativistic Plasmas Applied to Science, Energy, Industry, and Medicine", Kyoto, Japan, 30 May - 2 June 2011, ed. S. V. Bulanov, A. Yokoyama, Y. I. Malakhov, and Y. Watanabe) (Refereed proceedings paper).
DOI:10.1063/1.4737557

⑥.A. S. Pirozhkov, M. Kando, T. Zh. Esirkepov, P. Gallegos, H. Ahmed, E. N. Ragozin, A. Ya Faenov, T. A. Pikuz, T. Kawachi, A. Sagisaka, J. K. Koga, M. Coury, J. Green, P. Foster, C. Brenner, B. Dromey, D. R. Symes, M. Mori, K. Kawase, T. Kameshima, Y. Fukuda, L. Chen, I. Daito, K. Ogura, Y. Hayashi, H. Kotaki, H. Kiriyama, H. Okada, N. Nishimori, T. Imazono, K. Kondo, T. Kimura, T. Tajima, H. Daido, P. Rajeev, P. McKenna, M. Borghesi, D. Neely, Y. Kato, and S. V. Bulanov, "Soft-X-Ray Harmonic Comb from Relativistic Electron Spikes," *Phys. Rev. Lett.* **108** (13), 135004-5 (2012) (Refereed paper).
http://journals.aps.org/prl/abstract/10.1103/PhysRevLett.108.135004
DOI:10.1103/PhysRevLett.108.135004

⑦.A. S. Pirozhkov, M. Kando, T. Zh. Esirkepov, P. Gallegos, H. Ahmed, E. N. Ragozin, A. Ya. Faenov, T. A. Pikuz, J. K. Koga, H. Kiriyama, P. McKenna, M. Borghesi, K. Kondo, H. Daido, Y. Kato, D. Neely, and S. V. Bulanov, "Coherent x-ray generation in relativistic laser/gas jet interactions," [invited] *Proc. SPIE* **8140**, 81400A-16 (2011), (Proc. Int. Conf. X-Ray Lasers and Coherent X-Ray Sources: Development and Applications IX, Optics+Photonics Symposium, San Diego, USA, 23-25 August 2011, ed. J. Dunn and A. Klisnick) (Refereed proceedings paper).
DOI:10.1117/12.892898

〔学会発表〕（計　10　件）Presentations

①.A. S. Pirozhkov, [Invited presentation] "On-axis and off-axis high order harmonics generation by relativistic laser in gas jet target," *SPIE* **8849**, 8849-5 (2013), SPIE Optics+Photonics Symposium, International Conference on X-Ray Lasers and Coherent X-Ray Sources: Development and Applications X, 27th August 2013, San Diego, USA.

②.A. S. Pirozhkov, [Invited presentation] "High-Order Harmonic Comb from Relativistic Electron Spikes," CLEO-QELS QW1A.3 (2013), the Conference on Lasers and Electro-Optics CLEO:2013, 12th June 2013, San Jose, USA.
DOI:10.1364/CLEO_QELS.2013.QW1A.3

③.A. S. Pirozhkov, [Invited presentation] "New Coherent X-Ray Source Based on Relativistic High Harmonic Generation in Gas Jet Targets," III International Symposium "Topical Problems of Biophotonics – 2011," 18th July 2011, St. Petersburg – Nizhny Novgorod, Russia

〔その他〕

①.朝日新聞「超一瞬のＸ線　原理実証」平成24 年 3 月 15 日 p.25
Asahi Shimbun, "Ultrafast x-ray generation mechanism established," 15th March 2012, p.25 (in Japanese).

ホームページ等

①.Press-release on publication of Pirozhkov et al., *Phys. Rev. Lett.* **108** (13), 135004-5 (2012):
http://wwwapr.kansai.jaea.go.jp/press-2360.html

６．研究組織 Research Organization:

(1)研究代表者 Principle Investigator:

ピロジコフ　アレキサンダー
（PIROZHKOV, Alex）

独立行政法人日本原子力研究開発機構・原子力科学研究部門　量子ビーム応用センター・研究副主幹

Assistant Principal Researcher,
Quantum Beam Science Center,
Sector of Nuclear Science Research,
Japan Atomic Energy Agency

研究者番号 Researcher number: 00446410

(2)研究分担者 Co-Investigators: No

(3)連携研究者 Co-Investigators: No